

Molecular Orbital Studies of Hydrogen Bonds. III. C=O...H-O Hydrogen Bond in H₂CO...H₂O and H₂CO...2H₂O

Keiji Morokuma

Citation: *The Journal of Chemical Physics* **55**, 1236 (1971); doi: 10.1063/1.1676210

View online: <http://dx.doi.org/10.1063/1.1676210>

View Table of Contents: <http://aip.scitation.org/toc/jcp/55/3>

Published by the *American Institute of Physics*

Articles you may be interested in

[Energy decomposition analysis of covalent bonds and intermolecular interactions](#)

The Journal of Chemical Physics **131**, 014102 (2009); 10.1063/1.3159673

[A consistent and accurate ab initio parametrization of density functional dispersion correction \(DFT-D\) for the 94 elements H-Pu](#)

The Journal of Chemical Physics **132**, 154104 (2010); 10.1063/1.3382344

[Molecular-Orbital Studies of Hydrogen Bonds. An Ab Initio Calculation for Dimeric H₂O](#)

The Journal of Chemical Physics **48**, 3275 (2003); 10.1063/1.1669604

[Natural energy decomposition analysis: An energy partitioning procedure for molecular interactions with application to weak hydrogen bonding, strong ionic, and moderate donor-acceptor interactions](#)

The Journal of Chemical Physics **100**, 2900 (1998); 10.1063/1.466432

[Density-functional thermochemistry. III. The role of exact exchange](#)

The Journal of Chemical Physics **98**, 5648 (1998); 10.1063/1.464913

[A new local density functional for main-group thermochemistry, transition metal bonding, thermochemical kinetics, and noncovalent interactions](#)

The Journal of Chemical Physics **125**, 194101 (2006); 10.1063/1.2370993

**PHYSICS
TODAY**

**COMPLETELY
REDESIGNED!**

Physics Today Buyer's Guide
Search with a purpose.

Molecular Orbital Studies of Hydrogen Bonds. III. $C=O \cdots H-O$ Hydrogen Bond in $H_2CO \cdots H_2O$ and $H_2CO \cdots 2H_2O$

KEIJI MOROKUMA*

Department of Chemistry, University of Rochester, Rochester, New York 14627

(Received 27 August 1970)

Ab initio LCAO-MO-SCF calculation for $H_2CO \cdots H_2O$ is carried out with a minimal Slater basis set. The most stable conformation has an $O \cdots H$ distance of 1.89 Å with $\angle C=O \cdots H = -64^\circ$ and a stabilization energy of 3.5 kcal/mole, about a half of that for $H_2O \cdots H_2O$. Nonlinear and π hydrogen bonds, $H_2CO \cdots 2H_2O$ and the $O \cdots H-C$ hydrogen bond in $H_2O \cdots HCHO$, are also studied. An energy decomposition scheme is proposed and applied to $H_2CO \cdots H_2O$ and $H_2O \cdots H_2O$. In the latter the electrostatic energy 8.0 kcal/mole, the exchange repulsion -9.9 kcal/mole, the polarization and dispersion energy 0.3 kcal/mole, and the delocalization energy 8.2 kcal/mole are in good agreement with Coulson's estimates.

I. INTRODUCTION

Ab initio LCAO-MO-SCF calculations for hydrogen bonded systems between a neutral proton acceptor and a proton donor have first been carried out by Morokuma and Pedersen for dimeric $H_2O \cdots H_2O$ with a small Gaussian basis set,¹ and later for the same system and its polymeric analogs with various improved basis sets,²⁻⁵ and have been proved to provide a useful quantum mechanical insight to the nature of the hydrogen bonding. The calculations have been extended to other hydrogen bonds for combinations of HF, H_2O , and NH_3 .⁶

In many organic and biological systems the carbonyl group $>C=O$ is the most common base to form a hydrogen bond between a proton donor such as the $-OH$ and $>NH$ group.⁷ For instance, the hydration of carbonyl compounds clearly involves such an interaction. In polypeptides and polynucleotides the carbonyl group is by far the most important proton acceptor. One of the main differences between the $>C=O$ group and the oxygen atom in H_2O and alcohols is that the former possesses a well-defined π electron system. Experimentally the carbonyl $n \rightarrow \pi^*$ transition is found to make a large blue shift (1920 cm^{-1} for acetone in H_2O), while the $\pi \rightarrow \pi^*$ transition marks a smaller red shift.⁸

In the present paper we plan to carry out *ab initio* LCAO-MO-SCF calculations for the formaldehyde-water interaction. We hope that this system will serve as a model for a general consideration of the hydrogen bond to a carbonyl group. In Sec. II the theoretical method is explained, and a scheme for decomposing the hydrogen bond energy into various components is proposed. In Secs. III.A and III.B variations of the conformational angles and the $O \cdots H$ distance will be carried out to find the optimum dimer geometry for the linear hydrogen bonding. Sections III.C and III.D will handle the nonlinear and π hydrogen bond, respectively. In Sec. III.E a trimer $H_2CO \cdots 2H_2O$ will be considered. In Sec. III.F the $O \cdots H-C$ hydrogen bond in $H_2O \cdots HCHO$ will be examined. In Sec. IV the INDO method (a semiempirical LCAO-MO-SCF method) will be

applied to the problem and compared with *ab initio* results. In Sec. V the energy decomposition for $H_2O \cdots H_2O$ will be compared with Coulson's now classical estimate.

II. METHOD

A. Basis Functions and Geometry

In the *ab initio* SCF calculation the minimum Slater basis set is used with the POLYCAL program (an atomic orbital integral and SCF program package). The geometry and the orbital exponents are optimized for water and formaldehyde⁹ molecules, which are summarized in Table I. Since this basis set and geometry for the water molecule are identical to those used in $H_2O \cdots H_2O$ calculation,² we can make direct comparison between $H_2CO \cdots H_2O$ and $H_2O \cdots H_2O$.

In the interacting $H_2CO \cdots H_2O$ and $H_2CO \cdots 2(H_2O)$ system it is assumed that the monomer geometries are maintained. In most calculations (Secs. III.A, III.B, and III.E), one of the OH bonds of the water molecule is assumed to be directed to the aldehyde oxygen atom; in other words, the linear hydrogen bonding is assumed. The coordinate system used for such models are shown in Fig. 1. The formaldehyde molecule is fixed in the xy plane with the oxygen atom O_2 at the origin. The general conformation is obtained by the following four operations: (1) The water molecule is at first placed in the xy plane A with the H_1O_1 axis on the x axis and with the $O_1H_1^*$ axis pointing to the positive direction of y . (2) In the plane A rotate the H_2O molecule around the origin by an angle θ . (3) Then the plane A with H_2O on it is rotated around the y axis by an angle γ . Now the plane is called B . (4) At last the plane B is rotated around the H_1O_1 axis (M in Fig. 1) by an angle ϕ to give the plane C . The conformation of H_2CO-H_2O is now general and determined by the O_2H_1 distance $R_{O_2 \cdots H_1}$ and the angles θ , γ , and ϕ .

The semiempirical INDO calculations are also carried out with the program QCPE141.¹⁰

The hydrogen bond energy is the difference between the energy of isolated H_2CO and H_2O and the energy of

the $\text{H}_2\text{CO}\cdots\text{H}_2\text{O}$ and is positive when it results in a stabilization.

B. Decomposition of the Hydrogen Bond Energy

It is often convenient and instructive to decompose the hydrogen bond energy into various components, such as the electrostatic interaction, the polarization energy, the dispersion energy, the exchange interaction, and the charge transfer interaction.

Such an estimate has first been done by Coulson¹¹ for the water-water molecular interaction: the electrostatic energy +6 kcal/mole, the dispersion energy +3 kcal/mole, the (exchange) repulsion energy -8.4 kcal/mole, the delocalization energy $+8\pm 4$ kcal/mole, and the net hydrogen bond energy $+8.6\pm 4$ kcal/mole. Grahns used a simple quantum mechanical model to evaluate the electrostatic energy and the polarization energy.¹² Kollman and Allen has recently broke the hydrogen bond energy in two components, called the electrostatic and delocalization energy, respectively.¹³

Since the nomenclature of the contributions is often vaguely defined and confusing, first we would like to define them associated with appropriate wavefunctions.

At first the separated molecule A has the wavefunction $\alpha_{\Psi_A}^0$ and B has $\alpha_{\Psi_B}^0$ with the sum of the energy E_0 , where α is an antisymmetrizer. When the molecules approach, the following wavefunctions can be constructed:

(i) *The Hartree (nonantisymmetrized) product of isolated molecular wavefunctions.* The wavefunction is $\alpha_{\Psi_A}^0 \cdot \alpha_{\Psi_B}^0$ and the energy is E_1 . The two rigid molecules interact through the classical Coulomb forces.

TABLE I. Exponents and geometry parameters of monomeric H_2CO and H_2O used in $\text{H}_2\text{CO}\cdots\text{H}_2\text{O}$ calculation.

H_2O^a			
Optimized exponents		Optimized geometry	
H 1s	1.268	$R(\text{HO})$	1.85563 a.u. = 0.982 Å
O 1s	7.663	$\angle \text{HOH}$	101.07°
O 2s	2.250	Total energy	-75.70503 a.u.
O 2p	2.214		
H_2CO^b			
Optimized exponents		Optimized geometry	
H 1s	1.1833	$R(\text{HC})$	2.1164 a.u. = 1.120 Å
C 1s	5.6780	$\angle \text{HCH}$	118.0°
C 2s	1.7828	$R(\text{CO})$	2.2864 a.u. = 1.210 Å
C 2p	1.7128	Planar, symmetric	
O 1s	7.6630	Total energy	-113.47821 a.u.
O 2s	2.2385		
O 2p	2.2568		

^a Reference 2.

^b Reference 9.

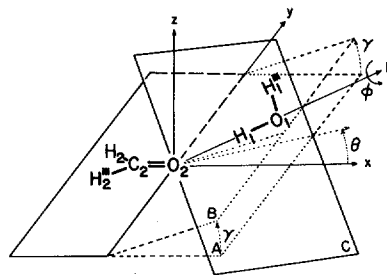


FIG. 1. Linear hydrogen bond model of $\text{H}_2\text{CO}\cdots\text{H}_2\text{O}$. The atoms O_2 , H_1 , and O_1 are collinear. See text on how to generate the figure.

(ii) *The Hartree product of two molecular wavefunctions which are individually optimized in the presence of the other molecule.* The wavefunction is $\alpha_{\Psi_A} \cdot \alpha_{\Psi_B}$ and the energy is E_2 . In the LCAO SCF approximation, this is accomplished by carrying out an SCF procedure by completely neglecting the differential overlap (including the resonance integrals) between AO's on the different molecules. Each molecule is polarized by the presence of the other molecule.

(iii) *The Hartree-Fock (antisymmetrized) product of two molecular wavefunctions.* $\alpha(\Psi_A^0 \Psi_B^0)$ and E_3 . In practice, MO's in Ψ_A^0 are not, in general, orthogonal to MO's in Ψ_B^0 . The same energy is calculated more simply by the wavefunction in which occupied MO's are orthogonalized to each other. The electron exchange between A and B is included in the calculation.

(iv) *The SCF wavefunction for the whole system* $\alpha_{\Psi_{AB}}$ and E_4 .

The difference between E_0 and E_1 is the electrostatic interaction energy E_{es} . $E_1 - E_2$ should be the polarization and dispersion interaction E_{pd} . These two terms, E_{es} and E_{pd} , are van der Waals interactions.¹⁴ The difference between E_1 and E_3 is the exchange interaction E_{ex} . This is negative, i.e., repulsive when two closed-shell molecules interact and is called the exchange repulsion. By going from E_3 to E_4 , the system gains polarization and dispersion energy E_{pd} as well as the charge transfer or electron delocalization E_{ct} between the two molecules. Similarly, $E_2 - E_4$ includes E_{ex} and E_{ct} . The charge transfer energy E_{ct} is thus obtained by $E_2 + E_3 - E_1 - E_4$. The "electrostatic energy" by Kollman and Allen seems to correspond to $E_0 - E_3$, which includes E_{es} and E_{ex} , their "delocalization energy" to $E_3 - E_4 = E_{pd} + E_{ct}$.

In the following sections we examine individual components E_{es} , E_{pd} , E_{ex} , and E_{ct} as well as the total hydrogen bond energy $\Delta E = E_0 - E_4$. Since the contributing E_{pd} was found relatively small (Sec. III.B) and the calculation of E_2 is time consuming, for most cases only the sum $E_{ct} + E_{pd}$ was obtained instead of separate E_{ct} and E_{pd} .

TABLE II. The angular dependency of the hydrogen bond energy, its components, and the charge transfer for $\text{H}_2\text{CO} \cdots \text{H}_2\text{O}$.^a

No.	Angles			Hydrogen bond energy ΔE	Components			Charge trans- fer ΔQ
	θ	γ	ϕ		E_{es}	E_{ex}	$E_{\text{et}} + E_{\text{pd}}$	
1	0	0	0	1.56				0.0243
2	0	0	90°	1.36	5.01	-9.05	5.40	0.0243
3	0	30°	0	1.42	4.67	-8.76	5.50	0.0228
4	0	30°	90°	0.94				0.0228
5	0	30°	-90°	1.71				0.0229
6	-15°	0	0	1.77	5.30	-9.14	5.61	0.0252
7	-30°	0	0	2.46	5.67	-9.36	6.15	0.0275
8	-30°	0	90°	2.28				0.0275
9	-30°	0	180°	2.10				0.0274
10	-30°	15°	0	2.19	5.30	-9.26	6.15	0.0269
11	-30°	30°	0	1.96	4.88	-9.01	6.09	0.0253
12	-30°	30°	90°	1.28				0.0253
13	-30°	30°	-90°	2.05				0.0253
14	-30°	30°	180°	1.44				0.0252
15	-45°	0	0	2.96	5.72	-9.61	6.85	0.0302
16	-60°	0	0	3.35	5.80	-9.78	7.34	0.0318
17	-60°	0	45°	3.15				0.0318
18	-60°	0	90°	2.71				0.0317
19	-60°	0	180°	2.02				0.0315
20	-60°	30°	0	2.55	5.10	-9.53	6.98	0.0291
21	-60°	30°	-90°	2.23				0.0290
22	-75°	0	0	2.99	5.81	-10.12	7.30	0.0310
23	-90°	0	0	0.24	5.95	-12.44	6.73	0.0267

^a The linear hydrogen bond with $R_{\text{O}_2 \cdots \text{H}_1} = 1.7963 \text{ \AA}$. All the energies are in kilocalories per mole. For the definition of angles, see Fig. 1.

The contribution of the correlation energy to the hydrogen bond was not considered at all in the present work.

III. RESULTS OF *AB INITIO* CALCULATIONS

A. Variations of Angles, θ , γ , and ϕ

At first we examine the effect of variation of three angles θ , γ , and ϕ for a fixed $\text{O}_2 \cdots \text{H}_1$ distance of

1.7963 Å, the most stable $\text{O}_2 \cdots \text{H}_1$ distance found for the H_2O dimer calculation with the same basis set. Table II shows the hydrogen bond energy and its components for various conformations. The angular dependency of the hydrogen bond energy is schematically shown in Fig. 2. Figure 2 can be regarded as a projection of the atoms O_1 and H_1^* (the external hydrogen of water molecule) onto the zy plane in which the H_2CO molecule is to be seen on the y axis with CO at the origin and with an H on each side.

Polynomial fits show that the most stable conformation has $\theta = -64^\circ$ (from Nos. 7, 15, 16, 22, and 23), $\gamma = 0^\circ$ (Nos. 16 and 20, and Nos. 7, 10, and 11), and $\phi = 0^\circ$ (Nos. 16, 17, and 18). At this conformation the H_2O molecule is in the plane of H_2CO molecule with the $\text{C}=\text{O} \cdots \text{H}$ angle of 116° . Experimentally in the formic acid crystal θ is -58° , and x-ray experiments in various acids ($\text{C}=\text{O} \cdots \text{HO}$) and amino acid ($\text{C}=\text{O} \cdots \text{HN}$) crystals gives quite a wide distribution of θ around -60° .¹⁵ As is shown in Fig. 3, the most stable $\text{H}_2\text{CO} \cdots$

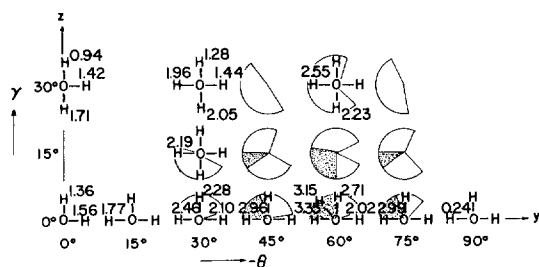


FIG. 2. Angular dependency of linear hydrogen bond energy. The abscissa is $-\theta$ and the ordinate is γ . The direction of O-H represents ϕ ; O-H corresponding to $\phi = 0^\circ$ and H-O to -180° . The figure can be regarded as a projection of the atoms O_1 and H_1^* (the external hydrogen of water molecule) onto the zy plane (Fig. 1) in which the H_2CO molecule is seen on the y axis (abscissa) with CO at the origin and with an H on each side. Conformations with $\Delta E \geq 3.35 - 0.60 = 2.75$ kcal/mole and $\Delta E \geq 3.35 - 1.20 = 2.15$ kcal/mole are shown with shadowy and open arcs, respectively.

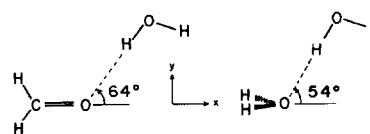


FIG. 3. Resemblance of the most stable geometry between $\text{H}_2\text{CO} \cdots \text{H}_2\text{O}$ and $\text{H}_2\text{O} \cdots \text{H}_2\text{O}$.

TABLE III. The $R_{O_2 \cdots H_1}$ and θ dependency of the hydrogen bond energy, its components, and charge transfer for $H_2CO \cdots H_2O$.^a

Angle θ	$R_{O_2 \cdots H_1}$ (Å)	Hydrogen bond energy ΔE	Components			Charge trans- fer ΔQ
			E_{es}	E_{ex}	$E_{et} + E_{pd}$	
-30°	1.4963	-2.73	13.33	-30.35	14.28	0.0633
-30°	1.7963	2.46	5.67	-9.36	6.15	0.0275
-30°	1.9463	2.69	3.88	-5.08	3.88	0.0171
-30°	2.0963	2.48	2.80	-2.73	2.41	0.0103
-30°	2.5000	1.69	1.59	-0.50	0.60	0.0023
-30°	3.5000	0.82	0.80	-0.01	0.03	0.0000
-60°	1.7963	3.35	5.80	-9.78	7.34	0.0318
-60°	1.9463	3.39	4.09	-5.30	4.60	0.0197
-60°	2.0963	2.99	3.02	-2.84	2.80	0.0118

^a The linear hydrogen bond with $\gamma = \phi = 0$. All the energies are in kcal/mole. For the definition of angles, see Fig. 1.

H_2O conformation is very similar to the $H_2O \cdots H_2O$ conformation, which, if the proton acceptor H_2O molecule is placed in the xz plane, has $\theta = -54^\circ$, $\gamma = 0^\circ$, and $\phi = 0^\circ$. The placement of H_2O in the xz plane leaves two sp^3 hybridized oxygen lone pairs in the xy plane, which have a maximum distribution at $\theta = \pm 55^\circ$, in agreement with $\theta = -54^\circ$ found above. In the $H_2CO \cdots H_2O$ system, on the other hand, the $C=O$ oxygen is supposed to have an sp^2 hybridization with a maximum at $\theta = \pm 60^\circ$, which is close to the calculated conformation $\theta = -64^\circ$.

The conformations accessible at $T = 300^\circ K$ are qualitatively shown by shadows in Fig. 2: $40^\circ < \theta < 78^\circ$ is allowed if ϕ and γ are at the minimum, $|\gamma| < 20^\circ$ if ϕ and θ are at the minimum, and $|\phi| < 90^\circ$ if θ and γ are at the minimum.

The examination of Table II shows that the stabilization from $\theta = 0$ to $\theta = -60^\circ$ is caused mainly by an increase of $E_{et} + E_{pd}$, while the destabilization from $\theta = -60^\circ$ to $\theta = -90^\circ$ is mainly due to a sharp increase of E_{ex} , and that the amount of charge transfer ΔQ is as expected closely related to $E_{et} + E_{pd}$ (Nos. 6, 7, 15,

TABLE IV. Comparison of $H_2CO \cdots H_2O$ and $H_2O \cdots H_2O$ hydrogen bonds.

	$H_2CO \cdots H_2O$	$H_2O \cdots H_2O^a$	Estimate ^b $H_2O \cdots H_2O$
Optimum geometry ^c			
$R_{O \cdots H}$	1.89 ₀ Å	1.79 ₆ Å	
θ	-63.9°	-53.8°	
Hydrogen bond energy ^d ΔE	3.45	6.55	8.6 ± 4
Components ^d			
E_{es}	4.64	8.00	6
E_{ex}	-6.71	-9.86	-8.4
E_{pd}	0.18	0.25	3
E_{et}	5.34	8.16	8 ± 4
Charge transfer ^e ΔQ	0.0237	0.0355	
Change in proton donor electron populations ^e			
H_1	-0.0186	-0.0295	
O 1s	0	0	
2s	-0.0038	-0.0051	
2p σ	+0.0333	+0.0493	
2p π	0	0	
H_1^*	+0.0127	+0.0207	

^a Geometry, ΔE , ΔQ , and populations are from Ref. 2.

^b By Coulson in Ref. 11.

^c $\phi = \gamma = 0$. For the nomenclature, see Fig. 1.

^d Energies at the optimum geometry in kcal/mole.

^e At the optimum geometry.

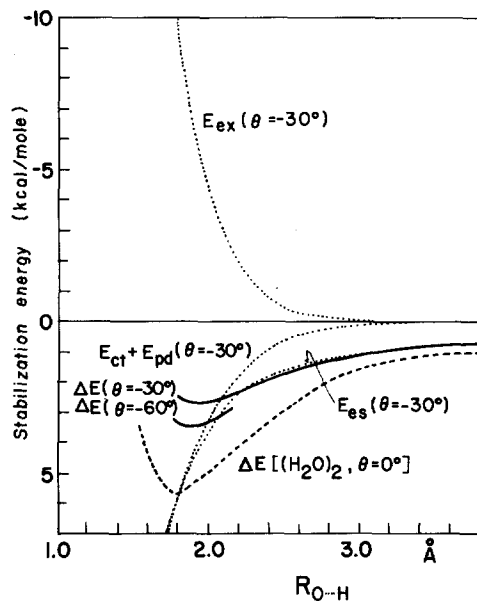


FIG. 4. The hydrogen bond energy and components as functions of $R_{O\cdots H}$. $\gamma = \phi = 0$. All curves are for $H_2CO\cdots H_2O$, unless specified for $(H_2O)_2$.

16, 22, and 23). The destabilization associated with the increase of γ from 0 is found to be essentially electrostatic (Nos. 7, 10, and 11 and Nos. 16 and 20).

A comparison of the $H_2CO\cdots H_2O$ results with that of $H_2O\cdots H_2O$ in Ref. 2 indicates that despite a smaller hydrogen bond energy the former has a sharper dependency than the latter.

B. Variation of $CO\cdots H$ Distance

By using $\gamma = \phi = 0$ determined in Sec. III.A, the hydrogen bond energy was calculated for a wide range of the $O\cdots H$ distance, $R_{O_2\cdots H_1}$ with $\theta = -30^\circ$ and -60° . The results are shown in Table III and Fig. 4. The interpolated minimum for $\theta = -60^\circ$ is found at $R_{O_2\cdots H_1} = 1.89 \text{ \AA}$ with $\Delta E = 3.42 \text{ kcal/mole}$ and for $\theta = -30^\circ$ at $R_{O_2\cdots H_1} = 1.95 \text{ \AA}$ with $\Delta E = 2.69 \text{ kcal/mole}$. From Table III and Sec. III.A we may conclude that with the present basis set the most stable $H_2CO\cdots H_2O$ complex is calculated to have an interpolated geometry $R_{O_2\cdots H_1} = 1.890 \text{ \AA}$, $\theta = -63.9^\circ$ and $\gamma = \phi = 0$ with a hydrogen bond energy $\Delta E = 3.45 \text{ kcal/mole}$.

The decomposition of ΔE for the $R_{O_2\cdots H_1}$ distance of

	2p π	-0.0300	+0.0300
-0.0104	1s	0	0
-0.0136	2s	+0.0047	-0.0045
	2p x	+0.0009	+0.0004
	2p y	+0.0117	-0.0128
<hr/>			
total σ		+0.0173	-0.0169
total		-0.0127	+0.0131

FIG. 5. Electron population change in the hydrogen bonded aldehyde molecule. $R_{O\cdots H} = 1.890 \text{ \AA}$, $\theta = -63.9^\circ$, and $\gamma = \phi = 0$. The positive value means more electron.

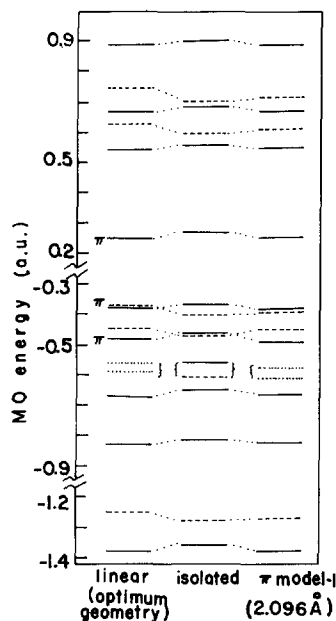


FIG. 6. Molecular orbital levels before and after hydrogen bonding. The solid lines are for formaldehyde MO's and broken lines for water MO's. The dotted lines indicate completely mixed MO's.

2.5 \AA or larger shows that the contribution of the electrostatic energy E_{es} is predominant, that $\Delta E \sim E_{es}$ because the other smaller contributions almost cancel out (i.e., $E_{ct} + E_{pd} \sim -E_{ex}$), and that the charge transfer ΔQ is very small. When the molecules approach to $R_{O_2\cdots H_1} \sim 2.1 \text{ \AA}$ the three components become almost identical in the magnitude. As the molecules become closer, the increase of $E_{es} + E_{ct} + E_{pd}$ surpasses the increase of the exchange repulsion, until the latter takes over the whole behavior.

The amount of electron population change at the optimum dimer geometry is shown in Table IV for the proton donor, H_2O and in Fig. 5 for the acceptor, H_2CO . The charge transfer takes place only for σ electrons but not at all for π electrons. The inclusion of a $p\pi$ vacant orbital on H_1 might induce a small π electron transfer.^{3,5} It is recognized that the population on the proton accepting O_2 atom is increased while the populations

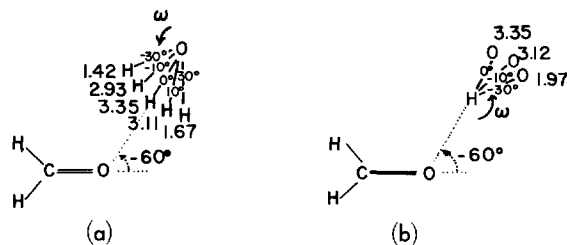


FIG. 7. Two models of the nonlinear hydrogen bond in $H_2CO\cdots H_2O$. In the Model a the $O_1\cdots O_2$ distance is fixed at the optimum with the $\theta = -60^\circ$ and the H_1-O_1 bond is rotated around O_1 . In the Model b the $O_2\cdots H_1$ distance is fixed at the optimum with $\theta = -60^\circ$ and the O_1-H_1 bond is rotated around H_1 . $\gamma = \phi = 0$. The external H^* , which follows the above rotation to maintain the monomer geometry, is omitted from the figure.

TABLE V. The nonlinear hydrogen bonds in $\text{H}_2\text{CO}\cdots\text{H}_2\text{O}$.^a

Model	Nonlinearity ω	Hydrogen bond energy ΔE , kcal/mole	Components			Charge trans- fer ΔQ
			E_{es}	E_{ex}	$E_{et}+E_{pd}$	
a	-30°	1.42	3.53	-5.38	3.27	0.0140
a	-10°	2.93	5.38	-9.11	6.67	0.0289
a	0°	3.35	5.80	-9.78	7.34	0.0318
a	$+10^\circ$	3.11	5.48	-9.00	6.64	0.0290
a	$+30^\circ$	1.67	3.45	-5.01	3.23	0.0142
b	-30°	1.97	5.72	-10.49	6.74	0.0296
b	-10°	3.12	5.74	-9.85	7.23	0.0315
b	0°	3.35	5.80	-9.78	7.34	0.0318

^a The models are shown in Fig. 7.

on H_2 , H_2^* , and C_2 are all decreased. The polarization of the π electron population makes the most important contribution to such a redistribution. The increase in the O_2 population was already found in the H_2O dimer¹ and cannot be expected if a fictitious $\text{O}\cdots\text{H}-\text{O}$ fragment is used in the calculation.

The MO energies at the optimum dimer geometry are compared in Fig. 6 with those for isolated H_2O and H_2CO molecules. All the MO's of H_2CO become more stabilized, while those of H_2O become less stabilized. This typical electron donor-acceptor behavior was observed also for $\text{H}_2\text{O}\cdots\text{H}_2\text{O}$.² The two MO's near -0.6 a.u. are so well mixed that an assignment to individual molecules is not possible, which is again similar to the $\text{H}_2\text{O}\cdots\text{H}_2\text{O}$ case.

At this point it is beneficial to compare the $\text{H}_2\text{CO}\cdots\text{H}_2\text{O}$ results with the $\text{H}_2\text{O}\cdots\text{H}_2\text{O}$ results in detail. A summary is compiled in Table IV. The $\text{O}\cdots\text{H}$ distance for $\text{H}_2\text{CO}\cdots\text{H}_2\text{O}$ is about 0.1 Å longer than $\text{H}_2\text{O}\cdots\text{H}_2\text{O}$, in coincidence with the weaker hydrogen bond of the former, i.e., ΔE is about 53% of the latter. The decomposition shows that E_{ex} and $E_{et}+E_{pd}$ for

$\text{H}_2\text{CO}\cdots\text{H}_2\text{O}$ are about two-thirds of those for $\text{H}_2\text{O}\cdots\text{H}_2\text{O}$, respectively, but E_{es} is only 58%. This means that the $\text{H}_2\text{CO}\cdots\text{H}_2\text{O}$ hydrogen bond at its optimum is slightly less ionic than $\text{H}_2\text{O}\cdots\text{H}_2\text{O}$ at its optimum. Table III shows that at $R_{\text{O}\cdots\text{H}}=1.7963$ Å $\text{H}_2\text{CO}\cdots\text{H}_2\text{O}$ has almost the same E_{ex} but quite less E_{es} and $E_{et}+E_{pd}$ than $\text{H}_2\text{O}\cdots\text{H}_2\text{O}$, resulting in a longer $R_{\text{O}\cdots\text{H}}$ and a weaker bonding.

The potential energy curve for $\text{H}_2\text{CO}\cdots\text{H}_2\text{O}$ inside $R_{\text{O}\cdots\text{H}}=3.0$ Å is found in Fig. 4 to be less steep than for $\text{H}_2\text{O}\cdots\text{H}_2\text{O}$. For instance, the energy ratio $\Delta E(\text{H}_2\text{CO}\cdots\text{H}_2\text{O})/\Delta E(\text{H}_2\text{O}\cdots\text{H}_2\text{O})$ is 67% at 3.5 Å, 59% at 2.5 Å and 53% near the minimum.

As one might well anticipate, the amount of charge transfer ΔQ is found to be proportional to E_{et} in the two systems, as well as the amount of change in atomic orbital electron populations of the proton donor (H_2O).

C. Nonlinear Hydrogen Bond

The hydrogen bonds in crystals are very often found to have almost linear $\text{X}\cdots\text{H}-\text{Y}$ structure, but small deviations from linearity are not uncommon.¹⁶

TABLE VI. The π -hydrogen bonds in $\text{H}_2\text{CO}\cdots\text{H}_2\text{O}$.

$R_{\text{H}\cdots\text{H}_2\text{CO}}$	ψ^a	Approach ^b	Hydrogen bond energy ΔE , kcal/mole	Components			Charge transfer ΔQ
				E_{es}	E_{ex}	$E_{et}+E_{pd}$	
1.7963	0	O	-2.49	3.23	-12.63	6.91	0.0310
2.0963	0	O	-0.04	1.24	-4.11	2.83	0.0131
2.0963	90°	O	-0.68				0.0131
2.0963	180°	O	-1.46				0.0131
2.3	0	O	0.33	0.72	-1.88	1.49	0.0069
2.5	0	O	0.40	0.50	-0.87	0.77	0.0035
2.8	0	O	0.30	0.30	-0.28	0.28	0.0012
2.3	0	C=O	-0.74	0.24	-2.62	1.64	0.0081
2.8	0	C=O	0.00 ₃	0.06	-0.38	0.32	0.0015
3.5	0	C=O	0.04 ₉	0.04	-0.03	0.03	0.0001

^a ψ is the angle of rotation of H_1^* around the O_1H_1 axis. For $\psi=0$ H_1^* is on the side opposite to CH_2 with respect to the O_1H_1 axis, while for $\psi=180^\circ$ H_1^* is on the same side.

^b For explanation, see Fig. 8.

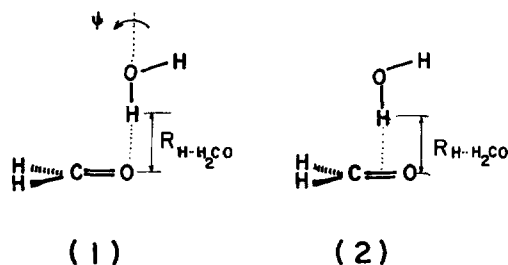


FIG. 8. Two models of the π hydrogen bond in $\text{H}_2\text{CO}\cdots\text{H}_2\text{O}$. The $\text{O}_1\text{--H}_1$ axis is perpendicular to the formaldehyde molecular plane. In Model 1 the $\text{O}_1\text{--H}_1$ approaches to the oxygen atom O_2 of formaldehyde, while in the Model 2 to the center of $\text{C}_2=\text{O}_2$ bond.

To examine the effect of nonlinearity, a most stable linear conformation $R = 1.7963 \text{ \AA}$, $\theta = -60^\circ$, $\gamma = \phi = 0$ is taken as a reference and a nonlinearity is introduced by rotating the H_2O molecule within its molecular plane by an angle ω . In Model a the rotation was around O_1 , and therefore the $\text{O}_2\cdots\text{O}_1$ distance is fixed. In Model b, on the other hand, it was around H_1 , the hydrogen bonded hydrogen atom (Fig. 7). The results are shown in Table V and Fig. 7.

In both models linear hydrogen bonds are found to be the most stable, but the nonlinearity up to $\pm 10^\circ$ can be accomplished without a serious loss of the hydrogen bond energy.

This $\pm 10^\circ$ altitude could help the formation of hydrogen bonds in which intramolecular or intermolecular geometrical restrictions do not allow a completely linear bonding.

The energy decomposition reveals quite a contrast between two models. In Model a all the three components decrease their magnitude drastically as the nonlinearity increases, while in Model b the nonlinearity destabilization is caused mainly by an increase in the exchange repulsion.

D. π Hydrogen Bonding

A weak interaction of an HO- or HN< group with a conjugated π electron system has been often observed experimentally in such systems as allyl alcohol and benzyl alcohol, and is called the π -hydrogen bonding.¹⁷ The π hydrogen bond energy is about 1–2 kcal/mole, considerably weaker than that of the regular hydrogen bond where an oxygen or nitrogen atom is proton acceptor.

TABLE VII. The hydrogen bond energy in $\text{H}_2\text{CO}\cdots 2\text{H}_2\text{O}$ and $\text{H}_2\text{CO}\cdots\text{H}_2\text{O}$.

Complex	Total energy ^a	Hydrogen bond energy ^a
$\text{H}_2\text{CO}\cdots 2\text{H}_2\text{O}$	-264.89764 a.u.	5.88 kcal/mole
$\text{H}_2\text{CO}\cdots\text{H}_2\text{O}$	-189.18864 a.u.	3.39 kcal/mole

^a At $\theta = -60^\circ$, $\gamma = \phi = 0$, and $R_{\text{O}\cdots\text{H}} = 1.9463 \text{ \AA}$.

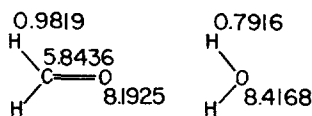


FIG. 9. Electron population in monomeric H_2CO and H_2O .

Since H_2CO has a π electron system, it would be suggestive in understanding π hydrogen bond in general to carry out a calculation for models in which OH of H_2O approaches perpendicularly to the H_2CO molecular plane. Two models were adopted as shown in Fig. 8, one with the HO bond approaching to O_2 , the aldehyde oxygen atom and the other approaching to the center of the aldehyde $\text{C}=\text{O}$ bond. The results are shown in Table VI.

The maximum hydrogen bond energy for the approach to O_2 is only about 0.4 kcal/mole at $R_{\text{H}\cdots\text{H}_2\text{CO}} = 2.5 \text{ \AA}$. The approach to the center of the $\text{C}=\text{O}$ bond gives only a slightly bound (~ 0.05 kcal/mole) potential curve. The calculated bond energy is smaller than the experimental estimates, 1–2 kcal/mole. This quite small π hydrogen bond energy may be related to the fact that the π electron system of formaldehyde is not a good electron donor because of the electronegativity of the oxygen atom. A comparison with Table III indicates that the π hydrogen bond gains as much or more charge transfer energy but suffers a larger exchange repulsion and a smaller electrostatic stabilization than the regular hydrogen bond at the same $\text{O}_2\cdots\text{H}_1$ distance. The electron acceptor-donor behaviors of MO levels are clearly recognized in Fig. 6.

E. Trimer $\text{H}_2\text{CO}\cdots 2\text{H}_2\text{O}$

The calculation in Sec. III.A shows that the dimer $\text{H}_2\text{CO}\cdots\text{H}_2\text{O}$ has a $\text{C}=\text{O}\cdots\text{H}$ angle 116.1° or $\theta = -63.9^\circ$. This conformation provides enough space for the second H_2O molecule approach to the carbonyl oxygen symmetrically but from the opposite side to the first H_2O . The approaches from other directions, such as the direction perpendicular to the formaldehyde molecular plane, the side of the first H_2O molecule, and the CH_2 side, are expected to be repulsive. Therefore, this symmetric approach seems to be the most stable form of interaction between a formaldehyde molecule and two H_2O molecules. This trimer would hopefully serve as a model of hydration of the carbonyl group in general.

An *ab initio* calculation for the symmetric trimer

TABLE VIII. The $\text{C-H}\cdots\text{O}$ hydrogen bond in $\text{H}_2\text{O}\cdots\text{HCHO}$.

$R_{\text{O}_1\cdots\text{H}_2}$ \AA	Hydrogen bond energy ΔE (kcal/mole)	Charge transfer ΔQ
1.9463	0.61	0.0249
2.5000	0.34	0.0039

TABLE IX. Comparison between *ab initio* and INDO calculations for $\text{H}_2\text{CO} \cdots \text{H}_2\text{O}$.

Method description	<i>Ab initio</i> optimized	INDO optimized	INDO near <i>ab initio</i> optimum
Geometry			
$R_{\text{O} \cdots \text{H}}$	1.89 Å	1.53 Å	1.80 Å
θ	-64°	0° (shallow minimum)	-60°
γ	0°	$\sim -30^\circ$ (small barrier)	0°
ϕ	0°	$\sim 90^\circ$ (almost free)	0°
ΔE	3.5 kcal/mole	9.6 kcal/mole	6.3 kcal/mole
Components ^a			
E_{es}	4.6	-19.0	-4.8
E_{ex}	-6.7	0	0
$E_{\text{et}} + E_{\text{pd}}$	5.5	28.6	11.1

^a In kcal/mole.

with $\theta = -60^\circ$, $\gamma = \phi = 0$ and $R_{\text{O} \cdots \text{H}} = 1.946$ Å (near the minimum for the dimer) was carried out. The results, shown in Table VII, indicate that the second hydrogen bond gains a stabilization energy 2.49 kcal/mole, as large as 73% of the first one. This trend is similar to the one observed in the calculations of water dimers and polymers.³⁻⁵ An obvious difference is that the water molecule, which may accept and at the same time donate protons, can form net or chain structures of hydrogen bonds, while formaldehyde participates as an acceptor of two protons without forming a net structure.

F. $\text{O} \cdots \text{H}-\text{C}$ Hydrogen Bond in $\text{H}_2\text{O} \cdots \text{HCHO}$

In the preceding sections we have implicitly assumed that H_2O is the proton donor to H_2CO . Is there any possibility of H_2CO being the proton donor to H_2O ? In a qualitative argument this is regarded as less likely because the C-H bond is less polar than the O-H bond (cf. Fig. 9), and only a weak hydrogen bond will be formed with the C-H group as a proton donor.¹⁸

To examine this point, we have carried out calculations for the $\text{H}_2\text{O} \cdots \text{HCHO}$ complex. The structure used is based on the most stable structure of water dimer (cf. Fig. 3) and is shown in Fig. 10. The results in Table VIII show that, as was expected, the $\text{C}-\text{H} \cdots \text{O}$ hydrogen bond is considerably weaker than the $\text{O}-\text{H} \cdots \text{O}$ hydrogen bond. It is noted that despite the small stabilization energy the amount of charge

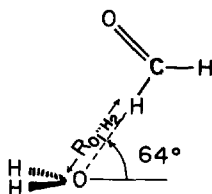
transfer from the proton acceptor to donor is considerably larger here than in the $\text{O}-\text{H} \cdots \text{O}$ hydrogen bond at the same distance (cf. Table III). From the population analysis (results not shown) one finds that the electron population increase in the proton donor (H_2CO) takes place on C, O, and the nonhydrogen bonded H and the decrease in the acceptor (H_2O) mostly takes place on the hydrogen atoms.

IV. RESULTS OF INDO CALCULATION

It has been found that the semiempirical CNDO/2 or INDO method gives a fair prediction of structures of hydrogen bonded complexes.¹⁹ To examine their applicability to $\text{H}_2\text{CO} \cdots \text{H}_2\text{O}$, a series of INDO calculations were carried out for the model of Fig. 1 with the monomer geometries of Table I and various values of $R_{\text{O} \cdots \text{H}}$, θ , γ , and ϕ . The optimized dimer structure is shown in Column 3 of Table IX, to be compared with *ab initio* results in Column 2. The $\text{O} \cdots \text{H}$ distance is much too small, as was found for other systems.^{19,20} The angular dependency even for this small $R_{\text{O} \cdots \text{H}}$ is very flat: no strong preference in the angles. This is in disagreement with the *ab initio* results which show a strong angular dependency.

The decomposition scheme was applied also to the INDO method. Because the differential overlaps between two molecules are completely neglected, $\alpha_{\Psi_A^0} \cdot \alpha_{\Psi_B^0}$ and $\alpha(\Psi_A^0 \Psi_B^0)$ give an identical energy; hence E_{ex} is always zero. Table IX shows that the electrostatic energy is repulsive. This is because in the INDO parametrization the core-core repulsion $6/R_{\text{O}_2 \cdots \text{H}_1}$ between O_2 and H_1 supersedes all the attractive contributions. This repulsion is compensated by a huge charge transfer or delocalization energy.

The strange decomposition behavior and the strange angular dependency warns that a care should be taken in applying the semiempirical method to the hydrogen bond problems.

FIG. 10. Geometry of $\text{H}_2\text{O} \cdots \text{HCHO}$ complex used in calculation.

V. DISCUSSION

It has been found in Sec. III.B that the $\text{H}_2\text{CO}\cdots\text{H}_2\text{O}$ hydrogen bond is longer and weaker than the $\text{H}_2\text{O}\cdots\text{H}_2\text{O}$ hydrogen bond. Experimental evidences for various $\text{C}=\text{O}\cdots\text{H}-\text{O}$ and $\text{H}-\text{O}\cdots\text{H}-\text{O}$ hydrogen bonds, though scattered, seem to confirm this as a general trend.²¹ At the same $R_{\text{O}\cdots\text{H}}$, say, 1.796 Å, $\text{H}_2\text{CO}\cdots\text{H}_2\text{O}$ has as much repulsion energy E_{ex} , only a slightly smaller delocalization energy E_{ct} but much less electrostatic energy E_{es} than $\text{H}_2\text{O}\cdots\text{H}_2\text{O}$. This is because the proton acceptor H_2CO of the former pair is less polar than that, H_2O , of the latter, as shown in Fig. 9. This could be generalized in that the enhanced polarity of the proton acceptor makes the hydrogen bond shorter and stronger.

The decomposition scheme proposed in Sec. II has been found quite useful in determining the nature of the hydrogen bond. It is interesting to compare our decomposition for $\text{H}_2\text{O}\cdots\text{H}_2\text{O}$ with an estimate made by Coulson.¹¹ Table IV indicates that the agreement between the two is remarkably good. Considering the fact that estimates of components were made from best available semiempirical or approximate quantum mechanical methods (the electrostatic energy by a statistical method by Pople,²² the dispersion forces from Slater–Kirkwood equation, the repulsion energy from Lennard–Jones potential,²³ and the delocalization energy from a valence bond calculation by Tsubomura²⁴), the agreement may not be surprising. We should keep in mind that the components are much more sensitive to the choice of the basis set as well as to the geometry of the complex than the total hydrogen bond energy is, and an improved basis set may well lead to somewhat different decomposition results.¹³

A theoretical study on the effect of the hydrogen bonding to the $n\rightarrow\pi^*$ and $\pi\rightarrow\pi^*$ excitation energies and their absorption intensities in $\text{H}_2\text{CO}\cdots\text{H}_2\text{O}$ is in progress in our laboratory.

VI. CONCLUSIONS

Ab initio calculations for the formaldehyde–water interaction with the minimum Slater basis set leads to the following conclusions:

(1) $\text{H}_2\text{CO}\cdots\text{H}_2\text{O}$ has the optimum geometry for the $\text{O}\cdots\text{H}$ distance of 1.89 Å with the hydrogen bond energy of 3.45 kcal/mole. This bonding is weaker and longer than the $\text{H}_2\text{O}\cdots\text{H}_2\text{O}$ hydrogen bonding, but the conformation of H_2O relative to the proton acceptor is remarkably similar in both cases.

(2) Nonlinear hydrogen bonds are weaker than the linear one, but a nonlinearity up to $\pm 10^\circ$ is achieved without loss of much energy.

(3) The π -hydrogen bond in $\text{H}_2\text{CO}\cdots\text{H}_2\text{O}$ is weak, with the hydrogen bond energy of 0.5 kcal/mole.

(4) A second H_2O molecule can form a hydrogen bond to $\text{C}=\text{O}$ with a substantial stabilization energy.

(5) The $\text{C}-\text{H}\cdots\text{O}$ hydrogen bond in $\text{H}_2\text{O}\cdots\text{HCHO}$ is weak ($\Delta E\sim 0.6$ kcal/mole).

(6) The quantum mechanical decomposition of the hydrogen bond energy in $\text{H}_2\text{O}\cdots\text{H}_2\text{O}$ agrees well with Coulson's estimate.

The INDO method predicts a much stronger, shorter, and less-angular-dependent (almost independent) hydrogen bond than the *ab initio* method does.

ACKNOWLEDGMENTS

The author would like to acknowledge Dr. R. M. Stevens for his POLYCAL program and J. R. Winick for his help in the early stage of the work. He would like to thank Dr. C. W. Kern and Dr. P. A. Kollman for helpful discussions. Most of the calculation was performed at the University of Rochester Computing Center which is in part supported by the National Science Foundation Grant GJ-828.

* Alfred P. Sloan Research Fellow, 1970–72.

¹ K. Morokuma and L. Pedersen, J. Chem. Phys. **48**, 3275 (1968), Paper I.

² K. Morokuma and J. Winick, J. Chem. Phys. **52**, 1301 (1970), Paper II.

³ P. A. Kollman and L. C. Allen, J. Chem. Phys. **51**, 3286 (1969).

⁴ J. Del Bene and J. A. Pople, Chem. Phys. Letters **4**, 426 (1970); J. Chem. Phys. **52**, 4858 (1970).

⁵ D. Hankins, J. W. Moskowitz, and F. H. Stillinger, J. Chem. Phys. **53**, 4544 (1970).

⁶ P. A. Kollman and L. C. Allen, J. Chem. Phys. **52**, 5085 (1970).

⁷ General references. (a) G. Pimentel and A. L. McClellan, *The Hydrogen Bond* (Freeman, San Francisco, 1960); (b) *Hydrogen Bonding*, edited by O. Hadzi (England, Pergamon, 1959); (c) W. C. Hamilton and J. A. Ibers, *Hydrogen Bonding in Solids* (Benjamin, New York, 1968).

⁸ Reference 7a, pp. 158–164.

⁹ K. Morokuma and J. H. Wu (unpublished results).

¹⁰ P. A. Dobosh, Quantum Chemistry Program Exchange No. 141, Indiana University, 1968.

¹¹ C. A. Coulson, Research (London) **10**, 149 (1957).

¹² R. Grahn, Arkiv Fysik **15**, 257 (1959).

¹³ P. A. Kollman and L. C. Allen (private communication) report the "electrostatic energy" of 4.50 kcal/mole and the "delocalization energy" of 3.05 kcal/mole for $\text{H}_2\text{O}\cdots\text{H}_2\text{O}$ at $R_{\text{O}\cdots\text{O}}=2.8$ Å and $\theta=\gamma=\phi=0$. These values are quite different from our $E_{\text{es}}+E_{\text{ex}}=-1.86$ kcal/mole and $E_{\text{pd}}+E_{\text{ct}}=8.41$ kcal/mole at $R_{\text{O}\cdots\text{H}}=1.80$ Å and $\theta=-54^\circ$. This discrepancy may be due to some difference in decomposition schemes or possibly due to the difference in basis functions.

¹⁴ (a) H. Margenau, Rev. Mod. Phys. **11**, 1 (1939); (b) J. O. Hirschfelder (Ed.), Advan. Chem. Phys. **12** (1967).

¹⁵ Reference 7a, p. 267.

¹⁶ Reference 7a, pp. 263–264; Ref 7c, pp. 162, 211, 260.

¹⁷ Reference 7a, pp. 190, 356.

¹⁸ Reference 7a, pp. 197–200.

¹⁹ A. S. N. Murthy and C. N. R. Rao, Theoret. Chim. Acta **13**, 81 (1968); Chem. Phys. Letters **2**, 123 (1968); P. S. Schuster and Th. Funck, Chem. Phys. Letters **2**, 587 (1968); P. A. Kollman and L. C. Allen, J. Am. Chem. Soc. **92**, 753 (1970).

²⁰ K. Morokuma, Chem. Phys. Letters **4**, 358 (1969).

²¹ Reference 7a, pp. 271, 278.

²² J. A. Pople, Proc. Roy. Soc. (London) **A205**, 163 (1957).

²³ E. J. Verwey, Rec. Trav. Chim. **60**, 887 (1941).

²⁴ H. Tsubomura, Bull. Chem. Soc. Japan **21**, 415 (1954).